Isotope fractionation pinpoints membrane permeability as barrier to atrazine biodegradation in Gram-negative *Polaromonas sp.* Nea-C

*Benno N. Ehrl[1], Mehdi Gharasoo[1], Martin Elsner[1,2]**

[1]Institute of Groundwater Ecology, Helmholtz Zentrum München, Ingolstädter Landstrasse 1, 85764 Neuherberg, Germany

[2]Chair of Analytical Chemistry and Water Chemistry, Technical University of Munich, Marchioninistrasse 17, 81377 Munich, Germany, m.elsner@tum.de

Published as "**Ehrl, B.**, **Gharasoo, M.**, **Elsner, M.**: Isotope fractionation pinpoints membrane permeability as a barrier to atrazine biodegradation in gram-negative *Polaromonas sp. Nea-C*. *Environ. Sci. Technol.* **52**, 4137-4144 (2018)", DOI: 10.1021/acs.est.7b06599

ABSTRACT: Biodegradation of persistent pesticides like atrazine often stalls at low concentrations in the environment. While mass transfer does not limit atrazine degradation by the Gram-positive *Arthrobacter aurescens* TC1 at high concentrations (> 1 mg·L^{-1}), bioavailability limitations have recently been observed at trace concentrations (< 0.1 mg·L^{-1}). To assess the bioavailability constraints on biodegradation, the roles of cell wall physiology and transporters remain imperfectly understood. Here, compound-specific isotope analysis (CSIA) demonstrates that cell wall physiology (i.e. the difference between Gram-negative and Gram-positive bacteria) imposes mass transfer limitations in atrazine biodegradation even at high concentrations. Atrazine biodegradation by Gram-negative *Polaromonas sp.* Nea-C caused significantly less isotope fractionation (ε(C) = -3.5 ‰) than expected for hydrolysis by the enzyme TrzN (ε(C) = -5.0 ‰) and observed in Gram-positive *Arthrobacter aurescens* TC1 (ε(C) = -5.4 ‰). Isotope fractionation was recovered in cell free extracts (ε(C) = -5.3 ‰) where no cell envelope restricted pollutant uptake. When active transport was inhibited with cyanide, atrazine degradation rates remained constant demonstrating that atrazine mass transfer across the cell envelope does not depend on active transport but is a consequence of passive cell wall permeation. Taken together, our results identify the cell envelope of the Gram-negative bacterium *Polaromonas sp.* Nea-C as relevant barrier for atrazine biodegradation.

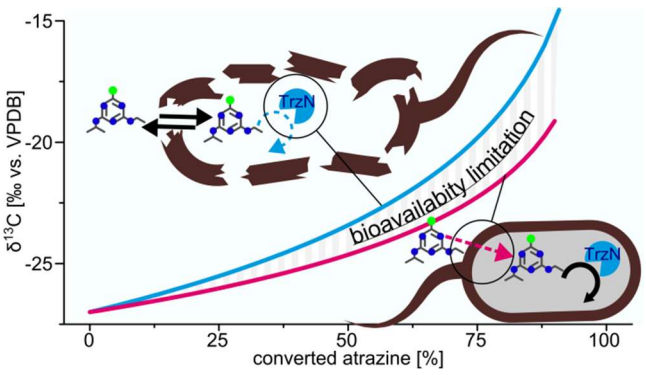

abstract art

Introduction

Groundwater contamination by micropollutants is a prominent challenge of our time. Since ground and surface waters represent an important drinking water resource, the presence of micropollutants is of concern not only for ecosystems, but also for human health.[1] Because of their ubiquitous release and their low concentrations, however, evaluating the fate of micropollutants in the environment is complex. Pharmaceuticals are discharged into the environment with wastewater treatment effluents[2-4] and pesticides used in agriculture even directly leach into groundwater on a large scale.[5, 6] EU regulations on drinking water quality set a maximum concentration of 0.1 µg/L for pesticides and their degradation products (European Union Drinking Water Directive, 98/83/EC). How difficult it is, however, to relate successful biodegradation in the lab to the fate of pesticides in the environment, is illustrated by the herbicide atrazine: even though banned in the EU as long ago as 2003, atrazine and its metabolites are still the groundwater contaminants most frequently detected above this threshold concentration.[7] The underlying bottlenecks of biodegradation at trace concentrations which cause this persistence have eluded researchers for years. Even though atrazine is initially adsorbed and retained to some extent on soil and sediments,[8] the pesticide becomes available at low concentrations (µg/L) for atrazine degrading bacteria.[9, 10] For such a situation, competing models claim that it is either mass transfer (uptake into microbial cells) which puts a limit to otherwise rapid enzymatic transformation,[11, 12] or that physiological limitations (enzyme activity, downregulation) prevail.[13] Compound-specific isotope analysis (CSIA) provides a way to directly visualize the rate-determining step of pollutant biodegradation:[14] Chemical bond breakage during pollutant degradation is slower when the bond contains a heavy isotope since the respective activation energy is higher. Therefore, the remaining pollutant molecules contain on average increasingly more heavy isotopes as an enzymatic

46 reaction proceeds.[15] This trend can be described by relating the change in isotope ratios
47 (R_t/R_o) to the fraction of the remaining pollutant *f* according to the Rayleigh equation[16, 17] (1)

$$\ln\left(\frac{R_t}{R_0}\right) = \varepsilon \times ln(f) \quad (1)$$

48 where the enrichment factor ε reflects the incremental isotope fractionation during
49 transformation. This isotope effect, however, can only be observed if substrate molecules
50 experiencing the isotopic discrimination during the enzymatic reaction in the cytosol diffuse
51 back out into the bulk solution, where the isotope ratio is assessed. Thus, any partially rate-
52 determining step preceding the irreversible enzymatic turnover (e.g. mass transfer) will lead
53 to a reduced exchange of "enriched" substrate molecules to the outside of the cell. As a
54 consequence, the observable isotope enrichment factor ε will be smaller, since the reduced
55 exchange masks the isotope fractionation of the enzymatic reaction.[18, 19] Masked isotope
56 fractionation due to mass transfer limitations is well understood from photosynthesis,[20, 21]
57 sulfate reduction,[22-24] or nitrate reduction.[25, 26] The same effect has previously been
58 demonstrated for organic pollutants taken up by active transport[27] and for non-polar
59 chlorinated ethenes.[19, 28] A conceptual framework has been brought forward by Thullner *et al.*
60 to mathematically predict the effect for passive permeation of organic pollutants through a
61 biological double membrane.[29, 30] Based on these studies, we recently discovered that cell wall
62 permeation was not relevant for atrazine biodegradation by *Arthrobacter aurescens* TC1 at
63 high concentrations, but became suddenly rate-limiting at low concentrations (low µg/L
64 range).[31] This finding is challenged by earlier observations by Meyer *et al.* that even at high
65 concentrations, isotope fractionation in atrazine degradation varied significantly between
66 bacterial strains catalyzing the same reaction.[32] Usually, the isotope fractionation factor is
67 assumed to be characteristic for a specific transformation pathway if the underlying enzyme
68 reaction is identical.[33-35] A compelling clue to explain the results of Meyer *et al.*, is, therefore,

69 the fact that differences exist between Gram-negative and Gram-positive bacterial strains. The
70 additional outer membrane in Gram-negative strains possibly constitutes an additional barrier
71 for mass transfer which can mask the enzymatic isotope fractionation. Indeed, Renpenning *et*
72 *al.* observed that carbon isotope fractionation during chlorinated ethene degradation differed
73 for Gram-positive and Gram-negative bacteria and depended on the integrity of the cell
74 envelope.[28] In the case of Meyer *et al.*, however, this proposed causal relationship could not
75 be uniquely pinpointed because different enzymes of the same family (AtzA vs. TrzN) were
76 involved. Consequently, it could not be excluded that the observed variability may,
77 alternatively, be attributable to subtle variations in transition state structures.
78 We, therefore, systematically addressed the question in our study by exploiting the
79 opportunity that the Gram-negative bacterium, *Polaromonas sp.* Nea-C, harbors the same set
80 of intracellular atrazine degrading enzymes[36] as the Gram-positive *A. aurescens* TC1 (TrzN,
81 AtzB, AtzC).[32, 37] Atrazine hydrolysis by TrzN (K_M = 19 μM, k_{cat} = 5.5 s^{-1}) proceeds via
82 initial protonation of the ring nitrogen and subsequent hydrolysis of the C-Cl bond.[36, 38]
83 Further, enrichment factors of the degradation reaction in whole cells are similar to those of
84 the degradation with purified TrzN without cell envelope meaning that atrazine degradation
85 by whole cells of Gram-positive *A. aurescens* TC1 is not mass transfer limited.[38] We
86 compared the isotope fractionation during atrazine degradation with intact cells of Gram-
87 negative *Polaromonas sp.* Nea-C – a scenario in which mass transfer across the cell envelope
88 can matter – relative to degradation with Gram-positive *A. aurescens* TC1, cell free extracts
89 of Gram-negative *Polaromonas sp.* Nea-C or purified TrzN enzyme,[38] three scenarios in
90 which mass transfer is absent. Furthermore, we addressed the possibility of active transport to
91 clarify whether passive membrane permeation of atrazine is sufficient to provide enough
92 influx for those bacteria to sustain growth. To this end, we investigated whether atrazine

degradation rates of *Polaromonas sp.* Nea-C and *A. aurescens* TC1 were affected when active transport was inhibited by the respiratory chain inhibitor potassium cyanide (KCN).

Experimental section

Chemicals

A list of chemicals used can be found in the supporting information.

Cultivation of bacteria

Polaromonas sp. Nea-C was kindly provided by Fabrice Martin-Laurent (Microbiologie du Sol et de l'Environnement, INRA, France) and *Arthrobacter aurescens* TC1 was kindly provided by Larry Wackett (The BioTechnology Institute, University of Minnesota, USA). All strains were grown in liquid mineral salt medium (MSM) containing a nitrogen source (composition see supporting information). Excess atrazine above the solubility limit was added in solid form to a concentration of 500 mg/L to provide enough nutrient for high cell densities. Cultures were incubated at room temperature (25°C).

Atrazine degradation with whole cells of *Polaromonas sp.* Nea-C for isotope analysis.

Growth of a freshly inoculated culture (500 mL) of *Polaromonas sp.* Nea-C was followed by monitoring the optical density (OD_{600}). During exponential phase (OD_{600} = 0.05) cells were pelleted by centrifugation (Heraeus Megafuge 40R, Thermo Scientific, TX-1000 rotor, 3700 *g*, 30 min, 4°C) and washed twice in 50 mL MSM to remove the remaining atrazine. After those washing steps, the cell pellet was resuspended in 500 mL of fresh MSM containing 30 mg/L atrazine. The atrazine concentration was close to the solubility limit of 33 mg/L (see media preparation in the SI) to maximize the amount of substance per volume and, hence, to minimize the necessary sample volume for reliable isotope analysis (see below).[39] The degradation experiment lasted approximately 24 h and the atrazine concentration was monitored by HPLC-UV (see below). For each of the three biological replicates, 5 samples for isotope analysis were taken (20 mL in the beginning and 50, 70, 150, 200 mL at

approximately 50 %, 75 %, 85 %, and 95 % atrazine consumption respectively). The degradation reaction was stopped by sterile filtration with a regenerated cellulose membrane filter (pore size 0.2 µm, diameter 47 mm; GE Healthcare ltd., UK). The biomass and the filter volume were not extracted, as their volume (< 0.5 mL) is negligible compared to the filtrate (> 20 mL). The filtrate was extracted three times with 10 % (v/v) dichloromethane. The combined dichloromethane extracts were evaporated under an air stream and the samples were reconstituted in 100 µL ethyl acetate for GC-IRMS measurements (see below).

Preparation of cell free extracts of *Polaromonas sp.* Nea-C.

Polaromonas sp. Nea-C cells were grown and harvested as described above. The cell pellet was resuspended in 5 mL of fresh MSM and put on ice. Cell membranes were disrupted in two passages by a French pressure cell (American Instrument Company, USA, 3/8" piston diameter, 20000 Psi). Remaining whole cells and cell fragments were removed by sterile filtration with a regenerated cellulose membrane filter (pore size 0.2 µm, diameter 47 mm; GE Healthcare ltd., UK) and the extract was stored on ice for a short time for the degradation experiment.

Atrazine degradation with cell free extracts of *Polaromonas sp.* Nea-C for isotope analysis.

The 5 mL concentrated cell free extract was diluted in 250 mL of fresh MSM containing 30 mg/L atrazine. The atrazine concentration over time was monitored by HPLC-UV (see below) by taking samples for 4 h. For each of the three biological replicates, 5 samples for isotope analysis were taken (10 mL in the beginning and 15, 35, 60, 120 mL at approximately 60 %, 80 %, 90 %, and 95 % atrazine consumption respectively) and the degradation reaction was stopped by extracting atrazine with three times 10 % (v/v) dichloromethane. The extracts were concentrated for GC-IRMS as described above.

Atrazine degradation rates with and without respiratory chain inhibitor KCN.

Growth of freshly inoculated cultures (50 mL) of both, *Polaromonas sp.* Nea-C and *A. aurescens* TC1, was followed by the OD_{600} and cell numbers per mL were estimated for both strains with $8 \cdot 10^8$ cells·mL^{-1}·OD_{600}. The cells were harvested as described above and the cell pellet was resuspended in 50 mL of fresh MSM. For both species, each of the three biological replicates was split in 2 x 25 mL cell suspensions to get the same biomass for the inhibited and the non-inhibited degradation experiment. To inhibit the respiratory chain, 0.25 mM KCN was added to one cell suspension. Afterwards, atrazine was added to both cell suspensions at a concentration of 3 mg/L. A small initial atrazine concentration was chosen to ensure short degradation times to rule out growth of the non-inhibited cells during the experiment. The atrazine concentration over time was monitored by HPLC-UV for 4 h (see below). Because *Polaromonas sp.* Nea-C and *A. aurescens* TC1 might have different TrzN abundances, we only compared each strain with and without inhibition and not the degradation kinetics of *Polaromonas sp.* Nea-C versus *A. aurescens* TC1.

Determination of the atrazine concentration by HPLC-UV.

Atrazine concentrations were measured using a Prominence HPLC system (Shimadzu Corp., Japan) together with a 100 x 4.6 mm Kinetex 5 µ Biphenyl 100 Å column equipped with a SecurityGuard ULTRA Biphenyl cartridge (both Phenomenex Inc., USA). The injected sample volume was 10 µL. Peak separation was achieved by 1 mL/min isocratic flow of a mixture of 51 % 5 mM KH_2PO_4 buffer at pH 7 and 49 % methanol, respectively, for 9 min. The compounds were detected by UV absorbance at 222 nm and the peaks were quantified using LabSolutions V 5.71 SP2 (Shimadzu Corp., Japan). External calibration was conducted with atrazine dissolved in 25 % methanol and 75 % water in the following concentrations: 0.5, 4, 12, 35 µg/L

Carbon and nitrogen isotope measurements with GC-IRMS

The method was adapted from Reinnicke *et al.*.[39] The GC-IRMS system consisted of a TRACE GC Ultra gas chromatograph (GC; Thermo Fisher Scientific, Milan, Italy) linked to a Finnigan MAT 253 isotope ratio mass spectrometer (IRMS) (Thermo Fisher Scientific, Germany) by a Finnigan GC Combustion III Interface (Thermo Fisher Scientific, Germany). Helium (grade 5.0) was used as carrier gas and the split injector was kept at 250°C with a 1:10 split at a flow rate of 1.4 mL/min. The samples were injected using a GC Pal autosampler (CTC, Switzerland) onto a 60-m DB-5 (30 m × 0.25 mm; 1 μm film; Restek GmbH, Germany) analytical column. Isotope values were determined as $\delta^{13}C$ and $\delta^{15}N$ values in per mill relative to Vienna PeeDee Belemnite (VPDB),[40] and Air-N_2.[41] The $\delta^{13}C$ and $\delta^{15}N$ values were assessed in relation to a monitoring gas (CO_2 and N_2, respectively) which was measured alongside each run at the beginning and the end. Calibration of monitoring gases was performed in a Finnigan MAT Delta S isotope ratio mass spectrometer with dual inlet system (Thermo Fisher Scientific, Germany). The gases were measured against VPDB and air, respectively, by use of international reference materials: the CO_2 gases RM 8562, RM 8563, and RM 8564 for CO_2 and NSVEC (N_2 gas) for N_2. Reference standards were provided by the IAEA. The GC oven started at 65 °C (hold 3 min), ramp 25 °C/min to 190 °C This was followed by a temperature ramp of 15 °C/min to 270 °C which was kept for 20 min.

Modelling of the isotope fractionation during the degradation.

In the absence of the cell envelope, the bioavailable concentration is equal to the bulk concentration. Therefore, the biodegradation of both substrate fractions (molecules containing ^{12}C and ^{13}C, short ^{12}S and ^{13}S) follows Michaelis-Menten kinetics[42] and is described by the set of equations (2) and (3):[16]

$$\frac{\mathrm{d}[^{12}\mathrm{S}]}{\mathrm{dt}} = \frac{q_{max}[^{12}\mathrm{S}]}{[^{12}\mathrm{S}] + [^{13}\mathrm{S}] + \mathrm{K_M}} \quad (2)$$

$$\frac{\mathrm{d}[^{13}\mathrm{S}]}{\mathrm{dt}} = \frac{\alpha q_{max}[^{13}\mathrm{S}]}{[^{12}\mathrm{S}] + [^{13}\mathrm{S}] + \mathrm{K_M}} \quad (3)$$

where α is the fractionation factor with ε = α-1, q_{max} is the maximum degradation rate, and K_M is the half saturation constant of the Michaelis-Menten kinetics. In the presence of mass transfer limitations across the cell envelope it is necessary to distinguish between substrate concentrations outside the cell, S, and substrate concentrations inside the cell, S(bio), where the exchange rate between these two phases is determined by the mass-transfer coefficient k_{tr}.[43, 44] Including the mass transfer limiting term in equation (2) and (3) gives equations (4) and (5) and analogous equations for the heavy fraction, where the last term in equation (5) is multiplied by the fractionation factor α:[26]

$$\frac{\mathrm{d}[^{12}\mathrm{S}]}{\mathrm{dt}} = -k_{tr}([^{12}\mathrm{S}] - [^{12}\mathrm{S(bio)}]) \quad (4)$$

$$\frac{\mathrm{d}[^{12}\mathrm{S(bio)}]}{\mathrm{dt}} = +k_{tr}([^{12}\mathrm{S}] - [^{12}\mathrm{S(bio)}]) - \frac{q_{max}[^{12}\mathrm{S}]}{[^{12}\mathrm{S}] + [^{13}\mathrm{S}] + \mathrm{K_M}} \quad (5)$$

These equations were solved and fitted to the experimental results to obtain the unknown parameters k_{tr} and the maximum degradation rate q_{max} using a modified version of ReKinSim.[45] The enzymatic fractionation factor α = ε + 1 was determined by the fit of the Rayleigh equation (Eq. (1), Table 1) and the value for K_M = 19 µmol/L was taken from the literature.[36] Equation (6) calculates an estimate of the atrazine diffusion coefficient in lipids, D_{lip},

$$\mathrm{D}_{lip} = \frac{k_{tr} \times \delta \times V}{A \times K_{lip-w}} \quad (6)$$

where δ = 10 nm is the thickness of two lipid double membranes (5 nm each) to mimic the Gram-negative cell wall and V = 0.5 L the volume of the cell suspension. A is the bacterial total surface area calculated from an estimate of 4×10^7 cells·mL^{-1} (derived from the OD_{600} =

206 0.05 with $8 \cdot 10^8$ cells·mL^{-1}·OD_{600}) and an average bacterial surface of 4 μm^3. K_{lipw} = 741 is
207 the lipid-water distribution coefficient of atrazine.[46]

208 **Results and discussion**

209 **Atrazine degradation with Gram-negative *Polaromonas sp.* Nea-C induced smaller**
210 **isotope fractionation than observed with TrzN.**

211 Resting cells of Gram-negative *Polaromonas sp.* Nea-C with a OD_{600} = 0.05 degraded 30
212 mg/L atrazine within 24 h (see **SI Figure S1**). TrzN-catalyzed atrazine hydrolysis to
213 hydroxyatrazine led to considerable isotope fractionation both for carbon (enrichment of ^{13}C
214 relative to ^{12}C corresponding to a normal isotope effect) and for nitrogen (depletion of ^{15}N
215 relative to ^{14}N representing an inverse isotope effect) (**Figure 1**). This inverse nitrogen
216 isotope effect is characteristic of proton-assisted hydrolysis in the transition state of TrzN.[38]
217 The enrichment factors for carbon ε(C) = -3.5‰ ± 0.1‰ and nitrogen ε(N) = 1.9‰ ± 0.1‰ (±
218 95 % confidence intervals) were determined by the Rayleigh equation, as shown in **Figure**
219 **2A, B**. These enrichment factors are significantly smaller than those described for atrazine
220 hydrolysis catalyzed by TrzN, i.e. those obtained during biodegradation with Gram-positive
221 *A. aurescens* TC1[32] (**Figure 2 A, B**). We screened for genes analogous to the *trzN* gene
222 sequence from *A. aurescens* TC1[47] in the NCBI database by Blast search[48] and found more
223 than 20 sequences coding for TrzN with more than 99 % similarity (**SI Table S1**). Also the
224 isotope fractionation of the abiotic model reaction – acid-catalyzed hydrolysis in water – is
225 stronger than observed in our experiment with *Polaromonas sp.* Nea-C.[32] Taken together, this
226 evidence is consistent with the hypothesis that a different rate determining step – mass
227 transfer across the cell envelope – partially masked the isotope fractionation of the enzyme in
228 *Polaromonas sp.* Nea-C. Remarkably, the enrichment factors for the Gram-negative
229 *Chelatobacter heintzii* (ε(C) = -3.7 ± 0.2 ‰ and ε(N) = 2.3 ± 0.4 ‰) are statistically
230 indistinguishable from *Polaromonas sp.* Nea-C. Both are Gram-negative bacteria with the

231 difference that *Chelatobacter heintzii* degrades atrazine with a different enzyme - AtzA[32]- but
232 still via the same acidic hydrolysis (**Table 1**). This raises the question whether these different
233 enzymes from different species (AtzA, TrzN from *Polaromonas sp.* Nea-C, and TrzN from *A.*
234 *aurescens* TC1) have different transition states and thus different enrichment factors, or
235 whether the difference in isotope fractionation is attributable to physiological differences in
236 the cell envelope that are characteristic of Gram-positive (*A. aurescens* TC1) versus Gram-
237 negative (*Chelatobacter heintzii* and *Polaromonas sp.* Nea-C) bacterial strains.

238 **Strong enzymatic isotope fractionation was masked by mass transfer limitations.**

239 Indeed, although the sequences of *trzN* genes from *Polaromonas sp.* Nea-C versus *A.*
240 *aurescens* TC1 are highly similar (see above), it cannot be strictly excluded that subtle
241 differences in the protein structure of even TrzN could be responsible for the differences in
242 isotope fractionation. For example, in a recent study by Schürner *et al.*.[38], we observed that
243 single point mutations in the *trzN* gene can lead to subtle changes in isotope fractionation. We
244 therefore prepared cell free extracts of *Polaromonas sp.* Nea-C to degrade atrazine to
245 hydroxyatrazine and followed the degradation with CSIA. As the hydrolysis of the atrazine C-
246 Cl bond does not depend on any cofactors or energy in the form of ATP, the cell free extracts
247 were highly active, atrazine turnover was fast (**SI Figure S2**), and was accompanied by strong
248 isotope fractionation, as shown in **Figure 1**. The isotope fractionation in cell free extracts was
249 considerably larger than in whole cells and gave enrichment factors $\varepsilon(C) = -5.3 \pm 0.7$ ‰ and
250 $\varepsilon(N) = 3.2 \pm 0.5$ ‰ that again were indistinguishable from those of *A. aurescens* TC1 (**Figure**
251 **2 A, B**).[32] This isotope fractionation was also similar to that of recombinant TrzN from *A.*
252 *aurescens* TC1 (instead of cell free extracts), and of abiotic acidic hydrolysis (**Table 1**).[32, 38]
253 Further, the slope of the dual element isotope plot $\lambda \approx \varepsilon(N)/\varepsilon(C)$ was the same for the
254 degradation with *Polaromonas sp.* Nea-C, *A. aurescens* TC1, and the cell free extract of
255 *Polaromonas sp.* Nea-C (λ = -0.55 ± 0.04, -0.60 ± 0.02, and -0.61 ± 0.14 respectively)

256 (**Figure 2 C**) and was similar to those with recombinant TrzN and abiotic acidic hydrolysis
257 (**Table 1**).[32, 38] This similarity in intrinsic isotope fractionation strongly suggests that the same
258 enzymatic reaction and same transition state prevailed but that this isotope fractionation was
259 partially masked by a non-isotope fractionating step. This masking occurred only in whole
260 cells with intact cell envelope, but not in cell free extracts of *Polaromonas sp.* Nea-C. Such
261 masking effects have previously be invoked to be attributable to (i) artificial high cell
262 densities[49], (ii) diffusion through water, or (iii) retention in extracellular polymeric substance
263 (EPS). These alternative explanations can be ruled out, however, since (i) our cell densities
264 were small in comparision with Kampara *et al.*'s study[49], (ii) the atrazine diffusion in water is
265 fast compared to diffusion in lipid membranes,[31] and (iii) *Polarmonas sp.* NeaC does not form
266 EPS. Consequently, we conclude that it was mass transfer across the cell envelope that was
267 the partially rate-limiting step in biodegradation of atrazine by the Gram-negative
268 *Polaromonas sp.* Nea-C, but not by the Gram-positive *A. aurescens* TC1.

269 **Passive processes dominate atrazine uptake into the cell.**

270 The phenomenon that organic pollutant uptake can mask isotope fractionation has already
271 been described by Qiu *et al.* where active transport along the proton motive force was the
272 rate-determining step for phenoxy acid degradation at high concentrations.[27] However, no
273 specific transporters for atrazine are known and non-polar molecules like atrazine with a
274 relatively high log P value of 2.6 can even permeate the phospholipid bilayer directly.[50, 51] A
275 phosphotransferase uptake system[52] can be ruled out, as atrazine does not undergo
276 phosphorylation. Other plausible uptake pathways are active transport across the lipid bilayer
277 driven by ATP hydrolysis or by an electrochemical gradient.[53-55] To explore these hypotheses,
278 atrazine degradation rates with *Polaromonas sp.* Nea-C and *A. aurescens* TC1, were
279 compared for both strains with and without addition of KCN. Cyanide is known to inhibit
280 cytochrome c so that the proton gradient collapses and ATP production ceases. As shown in

Figure 3, the initial atrazine degradation rates in *Polaromonas sp.* Nea-C and *A. aurescens* TC1 were not influenced by 0.25 mM KCN. We conclude that atrazine degradation does not depend on active transport by ATP or the proton motive force. Thus, passive processes driven by the atrazine gradient led to atrazine uptake, e.g. through facilitated transport with porins or permeation of the membrane itself. [51, 56] Note that we did not study isotope fractionation here, because (i) this concentration range was also covered in the previous degradation (**SI Figure S1**) and (ii) the isotope fractionation was not concentration dependent in this concentration range (**Figure 2A, B; Table 1**) so that the same isotopic enrichment factor is expected.

Implications for the application of CSIA in field studies.

When mass transfer masks the enzymatic reaction, this does not only limit biodegradation in the environment, but also has implications for the *in situ* assessment of biodegradation based on CSIA: pollutant turnover via the Rayleigh equation can best be estimated if isotope enrichment factors associated with a certain degradation pathway are constant and show little variation. However, as demonstrated in this study and by Renpenning *et al.*,[28] the isotope fractionation does not only depend on the reaction mechanism, but also on masking of the enzymatic reaction by mass transfer across the Gram-negative cell envelope. This leads to subtle differences in enrichment factors even for the same enzymatic reaction and introduces a small additional uncertainty in biodegradation assessments by CSIA in the field.[57] As a consequence, identification of the primary degradation pathway and the primary degrading strain would help to relate isotope fractionation in the field to isotope fractionation in the lab. A different strategy would be to use the enrichment factor determined under optimal conditions where mass transfer limitations are absent as a conservative estimate of biodegradation. This may underestimate biodegradation when the mass transfer becomes more and more rate limiting at low concentrations.[31] In contrast, the possibility to distinguish different processes and reaction pathways with dual element isotope plots remains valid, as

306 long as the mass transfer across the cell envelope does not mask the enzymatic isotope
307 fractionation completely.

308 Therefore, we theoretically analyzed how the isotope fractionation during atrazine
309 degradation by *Polaromonas sp.* Nea-C is affected by decreasing concentrations. This
310 concentration-dependent observable isotope enrichment factor ε* can be modeled with a
311 mathematical framework proposed by Thullner *et al.* for the case that mass transfer masks the
312 intrinsic enzymatic fractionation factor ε.[30] This framework correlates the specific affinity of
313 the enzyme $a = q_{max} \cdot K_M^{-1}$ with the mass transfer coefficient across the cell envelope k_{tr}. When
314 the influx (determined by k_{tr}) is slower than the enzymatic turnover (determined by *a*) the
315 fractionation factor ε will be masked which leads to a smaller observable enrichment factor ε*
316 (ε* < ε). We used numerical modeling (see experimental section above) to fit the time-
317 dependent enrichment in ^{13}C associated with the atrazine concentration decrease (equations
318 (4) and (5); SI Figure S3). Thus, we were able to estimate the parameters for Thullner *et al.*'s
319 model: $q_{max} = 2.7$ nmol $L^{-1}s^{-1}$ which gives $a = 0.14$ s^{-1} and the mass transfer coefficient across
320 the cell envelope $k_{tr} = 1.6 \cdot 10^{-4}$ s^{-1}. We validated our modeling approach for k_{tr} by calculating
321 the lipid diffusion coefficient D_{lip} according to equation (6) where the cell shape and
322 physiology is taken into account, to compare with literature values. Indeed, the calculated
323 atrazine lipid diffusion coefficient $D_{lip} = 1.3 \cdot 10^{-17}$ $m^2 \cdot s^{-1}$ was, as expected, smaller, but in the
324 same range as D_{lip} reported for atrazine in a single lipid bilayer of the Gram-positive *A.*
325 *aurescens* TC1.[31] This demonstrates, that our modeling approach yields realistic values for k_{tr}
326 allowing us to use k_{tr} to predict a decreasing observed fractionation factor ε* with decreasing
327 atrazine concentrations according to Thullner *et al.*.[30] Consistent with our experimental
328 results, at a concentration of 4 mg/L the enzymatic fractionation factor of ε = -5.3 ‰ is
329 already reduced to ε* = -3.5 ‰ and it is predicted to be further reduced to below -3 ‰ already
330 at an atrazine concentration of 1 mg/L.

Pollutant mass transfer of non-polar pollutants may be rate limiting for biodegradation in Gram-negative bacteria.

Our results strongly suggest that the specific physiology of the Gram-negative *Polaromonas sp.* Nea-C with its additional restrictive outer membrane limited the influx of atrazine. In contrast, isotope fractionation in the Gram-positive *A. aurescens* TC1 was fully observable, demonstrating the absence of mass transfer limitation. This shows that the permeation of the cell envelope is partially rate-determining for atrazine degradation by *Polaromonas sp.* Nea-C already at high concentrations. Furthermore, Renpenning *et al.* show that the mass transfer across the cell envelope of Gram-negative bacteria affects biodegradation of chlorinated ethenes.[28] Taken together, the difference between Gram-positive and Gram-negative physiology might also affect the nature of non-polar pollutant biodegradation in the environment: while a restrictive outer membrane protects Gram-negative bacteria from xenobiotics[58] and from the toxicity of compounds with high log P values[59, 60] it might also lower the supply of non-polar pollutants as nutrients when transporters are absent.

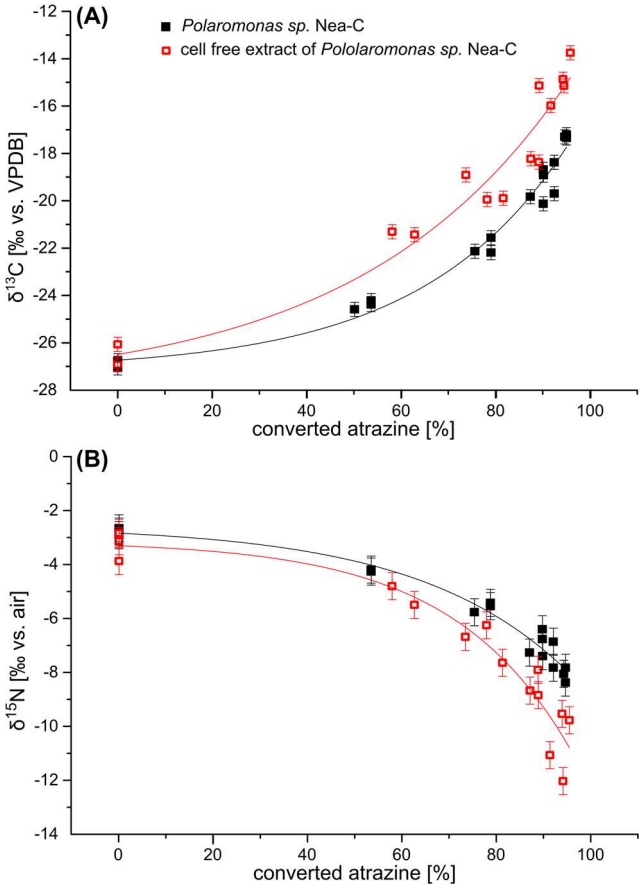

345

346 **Figure 1. Isotope fractionation in *Polaromonas sp.* NeaC depends on the integrity of the**
347 **cell envelope.** The biodegradation of atrazine by the Gram-negative *Polaromonas sp.* Nea-C
348 (black full squares) leads to considerably less isotope fractionation than the atrazine
349 degradation of cell free extracts of *Polaromonas sp.* Nea-C (red empty squares) both for
350 normal carbon **(A)** and inverse nitrogen **(B)** isotope fractionation. Error bars represent typical
351 standard deviations of carbon (± 0.3 ‰) and nitrogen (± 0.5 ‰) isotope analysis.

352

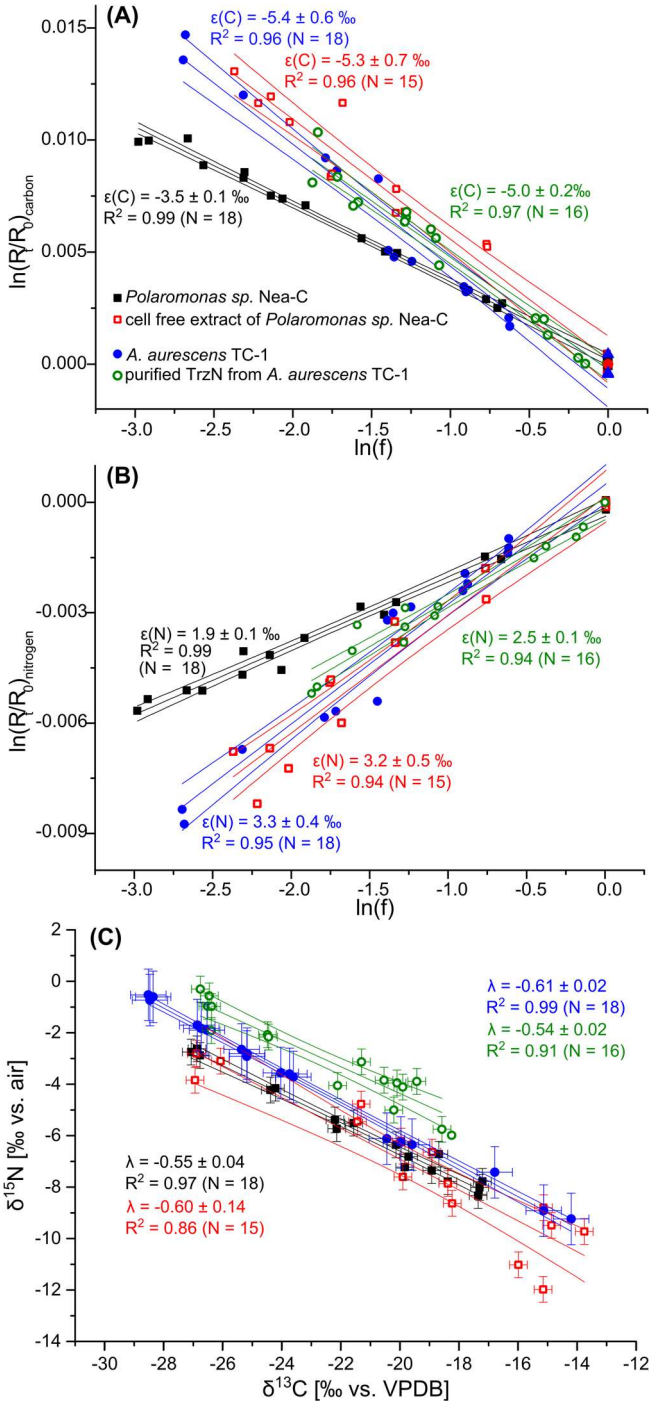

Figure 2. Rate limiting mass transfer across the Gram-negative cell envelope was revealed by isotope fractionation. Normal carbon isotope fractionation factors (ε(C)) **(A)** and inverse nitrogen isotope fractionation factors (ε(N)) **(B)** were determined by the Rayleigh equation. Enrichment factors in cell free extracts of *Polaromonas sp.* Nea-C (red empty squares) were identical to those with whole cells of Gram-positive *A.* aurescens TC1[32] (blue full circles) and purified TrzN[38] (green empty circles) indicating that an identical enzyme

360 reaction was at work. In contrast, smaller isotope fractionation was observed in degradation
361 with intact cells of Gram-negative *Polaromonas sp.* Nea-C (black full squares). **(C)** The slope
362 λ in the dual element isotope plot was similar for all degradation experiments, indicating that
363 a common reaction mechanism (acidic hydrolysis) and similar transition state architecture is
364 present in TrzN of both bacteria. Taken together, this indicates that the isotope effect of the
365 enzyme reaction was partially masked by mass transfer across the cell envelope in
366 *Polaromonas sp.* Nea-C. This non-fractionating step affects carbon and nitrogen fractionation
367 in the same way so that the dual element isotope slope λ stays constant even though the
368 enrichment factors are smaller. Error bars represent typical standard deviations of carbon
369 (± 0.3 ‰) and nitrogen (± 0.5 ‰) isotope analysis (except for data from degradation with *A.*
370 *aurescens* TC1 where total uncertainties are given).

371

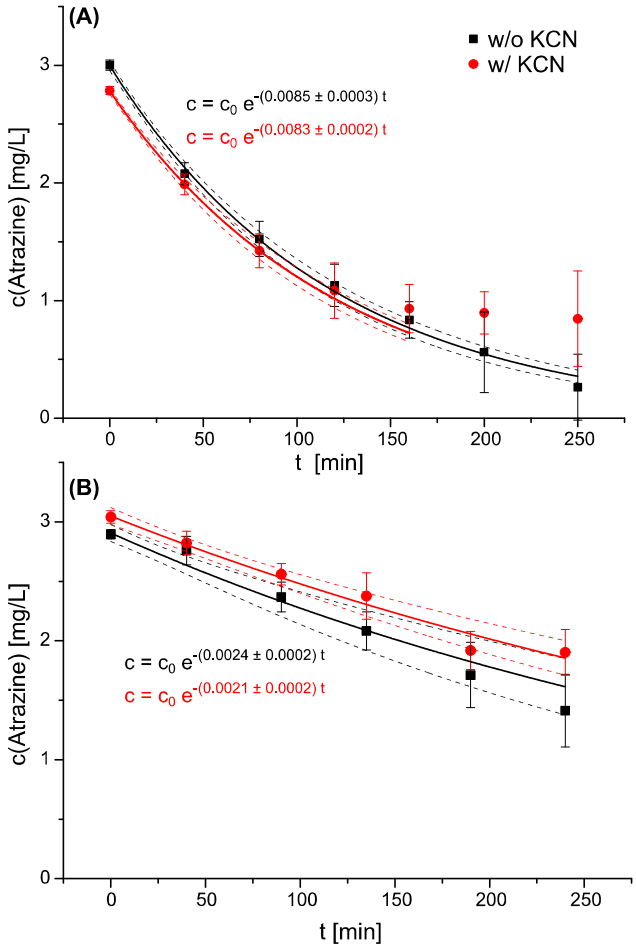

Figure 3. Mass transfer of atrazine into the cytosol is not mediated by a mode of active transport that depends on energy or the proton gradient. The degradation rates for both species ((A) *A. aurescens* TC-1 and (B) *Polaromonas sp.* Nea-C) were the same for control cells (black squares) and cells treated with 0.25 mM KCN (red circles). A pseudo first order reaction kinetics was assumed, as the concentration range was well below the Michaelis-Menten constant K_M of TrzN.[36] Cyanide was added to inhibit cytochrome c to prevent formation of a proton gradient so that energy production ceases. The hydrolytic enzyme TrzN does not depend on ATP or other cofactors and is not inhibited. The degradation rates were reduced in *A. aurescens* TC-1 150 minutes after KCN addition, indicating endogenous decay of TrzN. The fits of the first order rate constant in (A) and (B) are statistically not different at the 0.05 significance level.

385 **Table 1.** Overview of isotope fractionation during atrazine degradation via acidic hydrolysis

386 in different experimental setups. Uncertainties represent 95% confidence intervals.

experimental system	enzyme	Gram stain	ε(C) (‰)	ε(N) (‰)	λ ≈ ε(N)/ ε(C)	concentration (mg/L)	Ref.
whole cells *Polaromonas sp.* Nea-C	TrzN	negative	-3.5 ± 0.1	1.9 ± 0.1	-0.55 ± 0.04	30 - 1.4	this study
cell free extract *Polaromonas sp.* Nea-C	TrzN	negative	-5.3 ± 0.7	3.2 ± 0.5	-0.60 ± 0.14	30 - 2.8	this study
whole cells *A. aurescens TC1*	TrzN	positive	-5.4 ± 0.6	3.3 ± 0.4	-0.61 ± 0.02	18 - 1.3	[32]
purified *A. aurescens TC1* TrzN	TrzN	positive	-5.0 ± 0.2	2.5 ± 0.1	-0.54 ± 0.02	24 - 3	[38]
Chelatobacter heintzii	AtzA	negative	-3.7 ± 0.2	2.3 ± 0.4	-0.65 ± 0.08	15 - 1.8	[32]
abiotic pH 3 60°C	---	---	-4.8 ± 0.4	2.5 ± 0.2	-0.52 ± 0.04	24 - 3	[32]

387

388

389 ASSOCIATED CONTENT

390 **Supporting information**

391 A more detailed experimental section, graphs of the degradation experiments, and a table of
392 TrzN sequence similarities (PDF). This information is available free of charge via the Internet
393 at http://pubs.acs.org.

394 AUTHOR INFORMATION

395 **Corresponding Author**

396 *Chair of Analytical Chemistry and Water Chemistry, Technical University of Munich,
397 Marchioninistrasse 17, 81377 Munich, Germany, m.elsner@tum.de, +49 89 2180-78232

398 **Author Contributions**

399 The manuscript was written through contributions of all authors. All authors have given
400 approval to the final version of the manuscript.

401 **Funding Sources**

402 This work was funded by an ERC consolidator grant ("MicroDegrade", grant no. 616861)
403 awarded by the European Research Council.

404 **Acknowledgement**

405 This work was funded by an ERC consolidator grant ("MicroDegrade", grant no. 616861)
406 awarded by the European Research Council.

407 REFERENCES

408

409 1. Schwarzenbach, R. P.; Escher, B. I.; Fenner, K.; Hofstetter, T. B.; Johnson, C. A.; von
410 Gunten, U.; Wehrli, B., The Challenge of Micropollutants in Aquatic Systems. *Science* **2006,**
411 *313*, (5790), 1072-1077.

412 2. Dai, N.; Mitch, W. A., Relative Importance of N-Nitrosodimethylamine Compared to
413 Total N-Nitrosamines in Drinking Waters. *Environ. Sci. Technol.* **2013,** *47*, (8), 3648-3656.

414 3. Rosal, R.; Rodríguez, A.; Perdigón-Melón, J. A.; Petre, A.; García-Calvo, E.; Gómez,
415 M. J.; Agüera, A.; Fernández-Alba, A. R., Occurrence of emerging pollutants in urban
416 wastewater and their removal through biological treatment followed by ozonation. *Water*
417 *Research* **2010,** *44*, (2), 578-588.

418 4. Barbieri, M.; Carrera, J.; Ayora, C.; Sanchez-Vila, X.; Licha, T.; Noedler, K.; Osorio,
419 V.; Perez, S.; Koeck-Schulmeyer, M.; Lopez de Alda, M.; Barcelo, D., Formation of
420 diclofenac and sulfamethoxazole reversible transformation products in aquifer material under
421 denitrifying conditions: Batch experiments. *Science of the Total Environment* **2012,** *426*, 256-
422 263.

423 5. Battaglin, W. A.; Meyer, M. T.; Kuivila, K. M.; Dietze, J. E., Glyphosate and Its
424 Degradation Product AMPA Occur Frequently and Widely in U.S. Soils, Surface Water,
425 Groundwater, and Precipitation. *J. Am. Water Resour. Assoc.* **2014,** *50*, (2), 275-290.

426 6. Loos, R.; Locoro, G.; Comero, S.; Contini, S.; Schwesig, D.; Werres, F.; Balsaa, P.;
427 Gans, O.; Weiss, S.; Blaha, L.; Bolchi, M.; Gawlik, B. M., Pan-European survey on the

428 occurrence of selected polar organic persistent pollutants in ground water. *Water Research*
429 **2010,** *44*, (14), 4115-4126.

430 7. (LfU), B. L. f. U. *Pflanzenschutzmittel-Metaboliten Vorkommen und Bewertung:*
431 *Fachtagung des Bayerischen Landesamtes für Umwelt* 2008.

432 8. Selim, H. M., Modelling kinetic retention of atrazine and metribuzin in soil 1. *Soil*
433 *Science* **2004,** *169*, 25-34.

434 9. Morvan, X.; Mouvet, C.; Baran, N.; Gutierrez, A., Pesticides in the groundwater of a
435 spring draining a sandy aquifer: Temporal variability of concentrations and fluxes. *Journal of*
436 *Contaminant Hydrology* **2006,** *87*, (3-4), 176-190.

437 10. Graymore, M.; Stagnitti, F.; Allinson, G., Impacts of atrazine in aquatic ecosystems.
438 *Environ. Int.* **2001,** *26*, (7-8), 483-495.

439 11. Button, D. K.; Robertson, B.; Gustafson, E.; Zhao, X. M., Experimental and
440 theoretical bases of specific affinity, a cytoarchitecture-based formulation of nutrient
441 collection proposed to supercede the Michaels-Menten paradigm of microbial kinetics.
442 *Applied and Environmental Microbiology* **2004,** *70*, (9), 5511-5521.

443 12. Bosma, T. N. P.; Middeldorp, P. J. M.; Schraa, G.; Zehnder, A. J. B., Mass Transfer
444 Limitation of Biotransformation: Quantifying Bioavailability. *Environ. Sci. Technol.* **1997,**
445 *31*, (1), 248-252.

446 13. Wick, L. M.; Quadroni, M.; Egli, T., Short- and long-term changes in proteome
447 composition and kinetic properties in a culture of Escherichia coli during transition from
448 glucose-excess to glucose-limited growth conditions in continuous culture and vice versa.
449 *Environmental Microbiology* **2001,** *3*, (9), 588-599.

14. Hunkeler, D.; Elsner, M., Principles and Mechanisms of Isotope Fractionation. In *Environmental Isotopes in Biodegradation and Bioremediation*, Aelion, C. M.; Hohener, P.; Hunkeler, D.; Aravena, R., Eds. CRC Press: Boca Raton, London, New York, 2010.

15. Melander, L.; Saunders, W. H., *Reaction rates of isotopic molecules*. John Wiley: New York, 1980; p 331.

16. Hoefs, J., Theoretical and Experimental Principles. In *Stable isotope geochemistry*, 3rd ed.; Wyllie, P. J., Ed. Springer-Verlag: Chicago, 1987; pp 1-25.

17. Schmidt, H. L., Fundamentals and systematics of the non-statistical distributions of isotopes in natural compounds. *Naturwissenschaften* **2003,** *90*, (12), 537-552.

18. Northrop, D. B., The expression of isotope effects on enzyme-catalyzed reactions. *Annu. Rev. Biochem.* **1981,** *50*, 103-131.

19. Nijenhuis, I.; Andert, J.; Beck, K.; Kastner, M.; Diekert, G.; Richnow, H. H., Stable isotope fractionation of tetrachloroethene during reductive dechlorination by *Sulfurospirillum multivorans* and *Desulfitobacterium* sp. Strain PCE-S and abiotic reactions with cyanocobalamin. *Appl. Environ. Microbiol.* **2005,** *71*, (7), 3413-3419.

20. Farquhar, G. D.; Ehleringer, J. R.; Hubick, K. T., Carbon Isotope Discrimination and Photosynthesis. *Ann. Rev. Plant Physiol. Plant Mol. Biol.* **1989,** *40*, 503-537.

21. O'Leary, M. H., Carbon Isotopes in Photosynthesis. *Bioscience* **1988,** *38*, (5), 328-336.

22. Rees, C. E., A steady-state model for sulphur isotope fractionation in bacterial reduction processes. *Geochimica et Cosmochimica Acta* **1973,** *37*, (5), 1141-1162.

23. Brunner, B.; Bernasconi, S. M.; Kleikemper, J.; Schroth, M. H., A model for oxygen and sulfur isotope fractionation in sulfate during bacterial sulfate reduction processes. *Geochimica et Cosmochimica Acta* **2005,** *69*, (20), 4773-4785.

24. Wing, B. A.; Halevy, I., Intracellular metabolite levels shape sulfur isotope fractionation during microbial sulfate respiration. *Proceedings of the National Academy of Sciences* **2014,** *111*, (51), 18116-18125.

25. Kritee, K.; Sigman, D. M.; Granger, J.; Ward, B. B.; Jayakumar, A.; Deutsch, C., Reduced isotope fractionation by denitrification under conditions relevant to the ocean. *Geochimica et Cosmochimica Acta* **2012,** *92*, (0), 243-259.

26. Wunderlich, A.; Meckenstock, R.; Einsiedl, F., Effect of Different Carbon Substrates on Nitrate Stable Isotope Fractionation During Microbial Denitrification. *Environ. Sci. Technol.* **2012,** *46*, (9), 4861-4868.

27. Qiu, S.; Gözdereliler, E.; Weyrauch, P.; Lopez, E. C. M.; Kohler, H.-P. E.; Sørensen, S. R.; Meckenstock, R. U.; Elsner, M., Small 13C/12C Fractionation Contrasts with Large Enantiomer Fractionation in Aerobic Biodegradation of Phenoxy Acids. *Environ. Sci. Technol.* **2014,** *48*, (10), 5501-5511.

28. Renpenning, J.; Rapp, I.; Nijenhuis, I., Substrate hydrophobicity and cell composition influence the extent of rate limitation and masking of isotope fractionation during microbial reductive dehalogenation of chlorinated ethenes. *Environ. Sci. Technol.* **2015,** *49*, (7), 4293-4301.

29. Kampara, M.; Thullner, M.; Richnow, H. H.; Harms, H.; Wick, L. Y., Impact of Bioavailability Restrictions on Microbially Induced Stable Isotope Fractionation. 2. Experimental Evidence. *Environ. Sci. Technol.* **2008,** *42*, (17), 6552-6558.

493 30. Thullner, M.; Kampara, M.; Richnow, H. H.; Harms, H.; Wick, L. Y., Impact of
494 Bioavailability Restrictions on Microbially Induced Stable Isotope Fractionation. 1.
495 Theoretical Calculation. *Environ. Sci. Technol.* **2008,** *42*, (17), 6544-6551.

496 31. Ehrl, B. N.; Kundu, K.; Gharasoo, M.; Marozava, S.; Elsner, M., Rate limiting mass
497 transfer in micropollutant degradation revealed by isotope fractionation. *Nature Geoscience* **in**
498 **review, attached as supporting information for review only**.

499 32. Meyer, A. H.; Penning, H.; Elsner, M., C and N isotope fractionation suggests similar
500 mechanisms of microbial atrazine transformation despite involvement of different Enzymes
501 (AtzA and TrzN). *Environ. Sci. Technol.* **2009,** *43*, (21), 8079-8085.

502 33. Bernstein, A.; Ronen, Z.; Adar, E.; Nativ, R.; Lowag, H.; Stichler, W.; Meckenstock,
503 R. U., Compound-Specific Isotope Analysis of RDX and Stable Isotope Fractionation during
504 Aerobic and Anaerobic Biodegradation. *Environ. Sci. Technol.* **2008,** *42*, (21), 7772-7777.

505 34. Hunkeler, D.; Van Breukelen, B. M.; Elsner, M., Modeling Chlorine Isotope Trends
506 during Sequential Transformation of Chlorinated Ethenes. *Environ. Sci. Technol.* **2009,** *43*,
507 (17), 6750-6756.

508 35. Maier, M. P.; De Corte, S.; Nitsche, S.; Spaett, T.; Boon, N.; Elsner, M., C & N
509 Isotope Analysis of Diclofenac to Distinguish Oxidative and Reductive Transformation and to
510 Track Commercial Products. *Environ. Sci. Technol.* **2014,** *48*, (4), 2312-2320.

511 36. Shapir, N.; Pedersen, C.; Gil, O.; Strong, L.; Seffernick, J.; Sadowsky, M. J.; Wackett,
512 L. P., TrzN from Arthrobacter aurescens TC1 Is a zinc amidohydrolase. *J. Bacteriol.* **2006,**
513 *188*, (16), 5859-5864.

514 37. Devers, M.; Azhari, N. E.; Kolic, N.-U.; Martin-Laurent, F., Detection and
515 organization of atrazine-degrading genetic potential of seventeen bacterial isolates belonging
516 to divergent taxa indicate a recent common origin of their catabolic functions. *FEMS*
517 *Microbiology Letters* **2007,** *273*, (1), 78-86.

518 38. Schürner, H. K. V.; Seffernick, J. L.; Grzybkowska, A.; Dybala-Defratyka, A.;
519 Wackett, L. P.; Elsner, M., Characteristic Isotope Fractionation Patterns in s-Triazine
520 Degradation Have Their Origin in Multiple Protonation Options in the s-Triazine Hydrolase
521 TrzN. *Environ. Sci. Technol.* **2015,** *49*, (6), 3490-3498.

522 39. Reinnicke, S.; Juchelka, D.; Steinbeiss, S.; Meyer, A. H.; Hilkert, A.; Elsner, M., Gas
523 chromatography-isotope ratio mass spectrometry (GC-IRMS) of recalcitrant target
524 compounds: performance of different combustion reactors and strategies for standardization.
525 *Rapid. Commun. Mass. Sp.* **2012,** *26*, (9), 1053-1060.

526 40. Coplen, T. B., Guidelines and recommended terms for expression of stable-isotope-
527 ratio and gas-ratio measurement results. *Rapid Communications in Mass Spectrometry* **2011,**
528 *25*, (17), 2538-2560.

529 41. Coplen, T. B.; Krouse, H. R.; Boehlke, J. K., Reporting of nitrogen-isotope
530 abundances. *Pure & Applied Chemistry* **1992,** *64*, 907-908.

531 42. Michaelis, L. M., M.L., Die Kinetik der Invertinbindung. *Biochemische Zeitschrift*
532 **1913,** *49*, 333-369.

533 43. Gharasoo, M.; Centler, F.; Van Cappellen, P.; Wick, L. Y.; Thullner, M., Kinetics of
534 Substrate Biodegradation under the Cumulative Effects of Bioavailability and Self-Inhibition.
535 *Environ. Sci. Technol.* **2015,** *49*, (9), 5529-5537.

536 44. Best, J. B., The inference of intracellular enzymatic properties from kinetic data
537 obtained on living cells. I. Some kinetic considerations regarding an enzyme enclosed by a
538 diffusion barrier. *Journal of Cellular and Comparative Physiology* **1955,** *46*, (1), 1-27.

539 45. Gharasoo, M.; Thullner, M.; Elsner, M., Introduction of a new platform for parameter
540 estimation of kinetically complex environmental systems. *Environmental Modelling &*
541 *Software* **2017,** *98*, (Supplement C), 12-20.

542 46. Stenzel, A.; Goss, K. U.; Endo, S., Determination of Polyparameter Linear Free
543 Energy Relationship (pp-LFER) Substance Descriptors for Established and Alternative Flame
544 Retardants. *Environ. Sci. Technol.* **2013,** *47*, (3), 1399.

545 47. Mongodin, E. F.; Shapir, N.; Daugherty, S. C.; DeBoy, R. T.; Emerson, J. B.;
546 Shvartzbeyn, A.; Radune, D.; Vamathevan, J.; Riggs, F.; Grinberg, V.; Khouri, H.; Wackett,
547 L. P.; Nelson, K. E.; Sadowsky, M. J., Secrets of Soil Survival Revealed by the Genome
548 Sequence of Arthrobacter aurescens TC1. *PLoS Genetics* **2006,** *2*, (12), e214.

549 48. Zhang, Z.; Schwartz, S.; Wagner, L.; Miller, W., A Greedy Algorithm for Aligning
550 DNA Sequences. *Journal of Computational Biology* **2000,** *7*, (1-2), 203-214.

551 49. Kampara, M.; Thullner, M.; Harms, H.; Wick, L. Y., Impact of cell density on
552 microbially induced stable isotope fractionation. *Applied Microbiology and Biotechnology*
553 **2009,** *81*, (5), 977-985.

554 50. Endo, S.; Escher, B. I.; Goss, K.-U., Capacities of Membrane Lipids to Accumulate
555 Neutral Organic Chemicals. *Environ. Sci. Technol.* **2011,** *45*, (14), 5912-5921.

556 51. Parales, R. E.; Ditty, J. L., Substrate Transport. In *Handbook of Hydrocarbon and*
557 *Lipid Microbiology*, Timmis, K. N., Ed. Springer Berlin Heidelberg: Berlin, Heidelberg,
558 2010; pp 1545-1553.

559 52. Deutscher, J.; Francke, C.; Postma, P. W., How Phosphotransferase System-Related
560 Protein Phosphorylation Regulates Carbohydrate Metabolism in Bacteria. *Microbiology and*
561 *Molecular Biology Reviews* **2006,** *70*, (4), 939-1031.

562 53. Nichols, N. N.; Harwood, C. S., PcaK, a high-affinity permease for the aromatic
563 compounds 4-hydroxybenzoate and protocatechuate from Pseudomonas putida. *Journal of*
564 *Bacteriology* **1997,** *179*, (16), 5056-61.

565 54. Groenewegen, P. E.; Driessen, A. J.; Konings, W. N.; de Bont, J. A., Energy-
566 dependent uptake of 4-chlorobenzoate in the coryneform bacterium NTB-1. *Journal of*
567 *Bacteriology* **1990,** *172*, (1), 419-423.

568 55. Locher, H. H.; Poolman, B.; Cook, A. M.; Konings, W. N., Uptake of 4-toluene
569 sulfonate by Comamonas testosteroni T-2. *Journal of Bacteriology* **1993,** *175*, (4), 1075-1080.

570 56. Lambert, P. A., Cellular impermeability and uptake of biocides and antibiotics in
571 Gram-positive bacteria and mycobacteria. *Journal of Applied Microbiology* **2002,** *92*, 46S-
572 54S.

573 57. Mancini, S. A.; Hirschorn, S. K.; Elsner, M.; Lacrampe-Couloume, G.; Sleep, B. E.;
574 Edwards, E. A.; SherwoodLollar, B., Effects of Trace Element Concentration on Enzyme
575 Controlled Stable Isotope Fractionation during Aerobic Biodegradation of Toluene. *Environ.*
576 *Sci. Technol.* **2006,** *40*, (24), 7675-7681.

577 58. Delcour, A. H., Outer Membrane Permeability and Antibiotic Resistance. *Biochimica*
578 *et biophysica acta* **2009,** *1794*, (5), 808-816.

579 59. Sikkema, J.; de Bont, J. A.; Poolman, B., Mechanisms of membrane toxicity of
580 hydrocarbons. *Microbiological Reviews* **1995,** *59*, (2), 201-22.

581 60. Isken, S.; de Bont, J. A. M., Bacteria tolerant to organic solvents. *Extremophiles* **1998,**
582 *2*, (3), 229-238.

583

584